The Role of β-Sheet Interactions in Domain Stability, Folding, and Target Recognition Reactions of Calmodulin

J. Peter Browne, Molly Strom, Stephen R. Martin, and Peter M. Bayley*

Division of Physical Biochemistry, National Institute for Medical Research, The Ridgeway, Mill Hill, London NW7 1AA, U.K.

Received February 27, 1997; Revised Manuscript Received May 23, 1997[⊗]

ABSTRACT: Single-residue mutations have been made of the hydrophobic Ile or Val residue in position 8 of each of the four calcium-binding loop sequences (sites I−IV) of *Drosophila* calmodulin. These highly conserved residues are part of the hydrophobic core of either calmodulin domain and are involved in the structural link of two calcium-binding sites via a short antiparallel β-sheet. In the apo-form, the replacement of Ile (or Val) by Gly causes a significant destabilization, shown by the unfolding of the secondary structure of the domain carrying the mutation. In the presence of calcium, the deficiency in α-helical structure at 20 °C is restored for the mutants at site I, II, or III but not at site IV, which requires the further binding of a high-affinity target peptide to re-establish the native conformation. The extent of the destabilization is seen in the depression of the melting temperature of individual domains, which can be as large as 80 °C in the case of Ca_4-CaM(V136G). However, because of low values of the unfolding enthalpy for calmodulin domains, only relatively low values of <2 kcal/mol are implied for $\Delta\Delta G$, the free energy of destabilization due to mutation. Consistent with this, the secondary structure of any unfolded mutant domain is highly sensitive to solvent composition and is largely refolded in the presence of 12.5% (v/v) aqueous trifluoroethanol. Compared to wild-type calmodulin, the affinities of the mutants for calcium and target peptides from sk-MLCK at 20 °C are significantly reduced but the effects are relatively small. These results indicate that the conformation of calmodulin can be dramatically altered by mutation of a single highly conserved residue but that changes in solvent or the binding of a target sequence can readily compensate for this, restoring the wild-type properties. The results also suggest that the integrity of both the apo- and holo-forms of calmodulin is important for the maintenance of its biological function and confirm the importance of conserving the structural function of the residues involved in the β-sheet interactions.

The EF-hand is a well-defined characteristic structural motif of the family of calcium-binding proteins, of which calmodulin is a typical example (Klee, 1988; Strynadka and James, 1989; Falke et al., 1994). The motif comprises a helix−loop−helix sequence of 29 residues in which the calcium-binding functions are contained largely in the loop sequence (Marsden et al., 1990; Falke et al., 1994; Kawasaki & Kretsinger, 1994). The EF-hand is strongly conserved as a secondary structure element: the four EF-hands of calmodulin are known to be structurally very similar, with an rms difference of ≈1 Å for the α-carbon backbone atoms (Babu et al., 1988).

The sequence also shows strong conservation. Within the calcium-binding loop of eukaryotic calmodulins, residues in positions 1, 3, 5, 7, 9, and 12 are involved in coordination of the calcium ion. The Glu at position 12, which is the third residue of the F-helix, acts as a bidentate ligand for the calcium ion, and mutation of this residue in each site has been extensively studied (Haiech et al., 1991; Maune et al., 1992a,b; Starovasnik et al., 1992; Findlay et al., 1995a,b). Two noncoordinating residues are also strongly conserved, Gly at position 6 and the hydrophobic residue at position 8, which is predominantly Ile or Val (Falke et al., 1994). Even in nonfunctional EF-hands, position 8 is frequently a hydrophobic residue. EF-hands usually occur in pairs, linked back to back by a short antiparallel β-sheet. In calmodulin, this involves hydrogen bonding between residues I27/I63 (N-domain) and I100/V136 (C-domain). This β-sheet provides a direct structural link between the neighboring calcium-binding sites and is a likely candidate for the transmission of effects between pairs of sites such as the cooperativity of calcium binding, which occurs in both the N- and (especially) C-domains (Linse et al., 1991a). In each domain, the pair of hydrophobic residues associated with the β-sheet is within van der Waals contact and evidently contributes to the hydrophobic core of each domain. The core is itself of functional importance, since it is a major site for interaction of the domain with hydrophobic residues of the target sequences from the calmodulin-dependent proteins (Ikura et al., 1992; Meador et al., 1992, 1993). It is this area of each domain which becomes exposed in the activation reaction, when apo-calmodulin binds calcium ions, when the calcium-dependent conformational change results in a rearrangement of the four helices in each domain into a characteristic conformation (Finn et al., 1995; Kubinowa et al., 1995; Zhang et al., 1995). Calcium-saturated calmodulin presents hydrophobic surfaces into which two key hydrophobic residues of the target sequence can insert. In the case of a number of potentially amphiphilic α-helical target sequences, these key residues are 12 residues apart (Crivici and Ikura, 1995).

* To whom correspondence should be addressed. Phone: 0181-959-3666. Fax: 0181-906-4477. E-mail: p-bayley@nimr.mrc.ac.uk.

[⊗] Abstract published in *Advance ACS Abstracts,* July 15, 1997.

S0006-2960(97)00460-1 CCC: $14.00

In view of the specialized and highly conserved nature of the residue in position 8 of the binding loop, it is of interest to see the effects of point mutation of this position on the structure and function of calmodulin. We have therefore constructed four mutant *Drosophila* calmodulins in which this residue is replaced by glycine, giving CaM(I27G), CaM-(I63G), CaM(I100G), and CaM(V136G) (Browne et al., 1996, 1997). The choice of glycine was made on the basis that it is relatively low on the hydrophobic scale (Eisenberg et al., 1984), and is electrostatically neutral. Also, it can confer greater flexibility on the polypeptide backbone than any other residue. The conformation and thermal stability of the mutants have been assessed by near- and far-UV circular dichroism measurements; the functionality has been assessed by direct measurement of the calcium binding affinity of the mutants and by the affinity and conformational properties of the complex formed between the mutant calmodulin and synthetic peptides corresponding to the calmodulin binding sequence M13 derived from skeletal muscle myosin light chain kinase (sk-MLCK).

The results indicate that the replacement of Ile (or Val) by Gly causes a significant unfolding of the domain carrying the mutation in the apo-forms of all four mutant proteins. The deficiency in α-helical secondary structure of the mutants at 20 °C is restored in the presence of calcium for the mutation at site I, II, or III but not at site IV. The native conformation of the site IV mutant is only restored by the further binding of a high-affinity target peptide. The extent of the destabilization is seen in the depression of the melting temperature of individual domains, by at least 40 °C, in both the apo- and holo-forms. In spite of the magnitude of this effect, the affinity of the mutants for calcium and the affinity for a target peptide from sk-MLCK are only slightly reduced compared to wild-type calmodulin. These results indicate that the stability of calmodulin can be dramatically reduced by the mutation of a single highly conserved residue. These effects are discussed in terms of the contribution of key hydrophobic residues to the thermodynamic stability of the N- and C-domains of calmodulin.

MATERIALS AND METHODS

Mutagenesis. Cloning was performed as described by Sambrook et al. (1989) using enzymes from Boehringer Mannheim and *Escherichia coli* strain DH5α for all DNA manipulations. Custom oligonucleotides were synthesized on a Beckmann Oligo 1000 DNA synthesizer. Mutagenesis was facilitated by transferring the wild-type CaM cDNA as a *Nco*I/*Xba*I fragment from pOTSNco12 (Maune et al., 1992a), with the *Nco*I site filled in, into the *Sma*I/*Xba*I sites of pBSIISK$^+$ (Stratagene). The desired mutations were introduced with a two-step PCR-directed mutagenesis approach (Landt et al., 1990) using a custom oligonucleotide carrying the appropriate base pair mismatches in combination with the pBSSIISK$^+$ 'reverse' and '−20' primers. The sequence of the entire coding region of each mutant was verified using the Sequenase v2.0 kit (USB). For protein expression, the CaM cDNA's were transferred back to the pOTSNco12 as a *Nco*I/*Xba*I fragment.

Protein Expression and Purification. Bacterial cell cultures (6 L), AR68 for wild-type and AR58 for the mutants, were harvested after heat shock treatment as described by Shatzman and Rosenberg (1986). Cells were resuspended in 25 mM Tris/HCl, 50 mM NaCl, 1 mM $CaCl_2$, 1 mM PMSF (pH 7.5) and broken by sonication at maximum output on 50% cycle with a Vibra Cell Sonicator (Sonics and Materials, Danbury, CT). An initial purification was carried out using phenyl sepharose (Pharmacia) in a modification of the procedure of Putkey et al. (1985). The supernatant, after centrifugation at 100000*g* for 20 min at 4 °C, was made to 500 mM in KCl and passed over a 200 mL phenyl sepharose column equilibrated in 25 mM Tris/HCl, 500 mM KCl, 1 mM $CaCl_2$ (pH 7.5). The column was washed with three column volumes of the equilibration buffer, and the CaM was eluted with 25 mM Tris/HCl, 500 mM KCl, 5 mM EDTA (pH 7.5). Fractions containing CaM were concentrated to 10 mL using the Amicon Diaflow system with a 10 kDa cutoff membrane and further purified by gel filtration on a Sephadex G75 column (Pharmacia; 100 × 2.6 cm column, 0.25 mL/min flow rate) equilibrated with 25 mM Tris/HCl, 100 mM KCl, 1 mM $CaCl_2$ (pH 7.5). The V136G and I63G preparations contained small amounts of proteolytic fragments of CaM. Intact CaM was separated from these fragments and purified to homogeneity by ion exchange chromatography on a 5/5 Mono Q column (Pharmacia) with a 40 min 50−500 mM KCl gradient in 25 mM Tris/HCl with 1 mM $CaCl_2$ (pH 7.5). The purified proteins ran as single bands on SDS−PAGE (15% gel, Laemmli system) and were further checked for purity on a VG Platform electrospray mass spectrometer using on-line trapping, as described by Aitken et al. (1995).

Calmodulin samples for Ca titration were made calcium free by treating with 5 mM EGTA and then desalting by passage though two Pharmacia PD10 (G25) columns equilibrated with Chelex-treated buffer (25 mM Tris, 100 mM KCl, pH 8.0). Residual calcium concentration in the buffer was estimated as 0.4−0.6 μM using 5,5′-Br_2BAPTA.

Peptides. The peptides WFF (NH_2-KKRWKKNFIA-VSAANRFK-CO_2H, residues 1−18 of the M13 target sequence), FFF (WFF with a W4F substitution), FWF (WFF with W4F and F8W substitutions), FFW (WFF with W4F and F17W substitutions), and CBP1 (CH_3CO-LKLKKLL-KLLKKLLKLG-NH_2) were synthesized on an Applied Biosystems 430A peptide synthesizer and purified by HPLC on a C18 column. Concentrations of the Trp-containing peptides and the wild-type calmodulin were determined spectrophotometrically using $\epsilon_{280nm} = 5690\ M^{-1}cm^{-1}$ for the WFF, FWF, and FFW peptides (Gill and von Hippel, 1989), $\epsilon_{259nm} = 585\ M^{-1}cm^{-1}$ for the FFF peptide (Gill and von Hippel, 1989), and $\epsilon_{279nm} = 1578\ M^{-1}cm^{-1}$ for Ca_4-CaM-(WT) (Maune et al., 1992a). The extinction coefficients for the mutants were estimated as described in the Results section. All measurements of absorption spectra were made on a Cary 3E spectrophotometer at 20 °C.

Fluorescence Measurements. Uncorrected tryptophan fluorescence emission spectra were recorded using a SPEX FluoroMax fluorimeter with excitation at 280 or 290 nm (bandwidth 1.7 nm) and emission scanned from 300 to 450 nm (bandwidth 5 nm). Spectra were recorded at 20 °C in UV-transmitting plastic cuvettes. The buffer was 25 mM Tris, 100 mM KCl, pH 8.0, unless otherwise noted, and protein/peptide concentrations were in the range 1−2.5 μM.

Circular Dichroism Measurements. CD spectra were recorded in 25 mM Tris, 100 mM KCl at pH 8.0 using a

Jasco J-600 spectropolarimeter, with protein concentrations of 7.5 μM (far-UV, 1 mm path length) or 100−150 μM (near-UV, 10 mm path length) as described elsewhere (Martin et al., 1995). Spectra are presented as the CD absorption coefficient calculated using the molar concentration of peptide or protein ($\Delta\epsilon_M$), rather than on a per residue basis ($\Delta\epsilon_{MRW}$), in order to facilitate direct comparison of free proteins, peptides, and protein:peptide complexes. Values of $\Delta\epsilon_{MRW}$ can be obtained by dividing $\Delta\epsilon_M$ by the appropriate number of peptide bonds (147 for CaM and $n - 1$ for an n residue peptide).

Thermal Stability. CD changes as a function of temperature were studied in 10 mm cuvettes with direct monitoring of the temperature in the cuvette using a Comark electronic thermometer. The measurements were made at protein concentrations of ≈7.5 μM (far-UV) or 150 μM (near-UV). The buffer contained either 1 mM (or 5 mM) $CaCl_2$ or 1 mM EGTA. Heating rates of ∼1 °C/min were used over the range 5−82 °C. All the thermal unfolding profiles reported here were 95−99% reversible. Where the full transition amplitude could be recorded, approximate values of the enthalpy of unfolding were estimated from a two-state van't Hoff analysis.

Determination of Peptide Affinities. Peptide affinities were determined by direct fluorometric titration as described in Findlay et al. (1995a). Typically, 0.8 μM peptide in 25 mM Tris, 100 mM KCl, 1 mM $CaCl_2$ (pH 8.0) at 20 °C was titrated with aliquots of concentrated CaM solution (wild-type or mutant), and the fluorescence emission intensity at 332 (or 334) nm was recorded (λ_{ex} = 290 or 295 nm). At least three independent determinations were performed, and the average values for K_d (derived from a standard least-squares fitting procedure applied to the raw experimental data) are reported with standard deviations. Values of $K_d \leq 1$ nM are determined using peptide concentrations down to 0.1 μM with integration of the fluorescence signal and low excitation light levels to avoid photobleaching.

Stopped-Flow Measurements. Kinetic experiments were performed on a Hi-Tech SF61-MX stopped flow spectrophotometer as described (Bayley et al., 1996; Brown et al., 1997). The temperature was 20 °C and the buffer was 25 mM Tris, 100 mM KCl (pH 8.0). Fluorescence signals (λ_{ex} = 334 nm; with emission through a 370 nm cut-on filter) were recorded following stopped-flow mixing of 3 μM Ca_4-CaM(WT) (or mutant CaM) plus 25 μM free calcium with an equal volume of 90 or 150 μM Quin-2. At least eight traces were recorded for each mixture in each experiment, and at least three independent experiments were performed for each combination of CaM and chelator. The individual traces were analyzed using the Hi-Tech software. A single exponential fit was adequate in all cases (as judged by inspection of χ^2 values and randomness of the residuals).

Calcium Binding Studies. Stoichiometric calcium binding constants, K_1 to K_4, for the calmodulin mutants were determined from calcium titrations performed in the presence and absence of the WFF peptide, using the chromophoric calcium chelator 5,5′-Br_2BAPTA as described (Linse et al., 1988, 1991a; Martin et al., 1995). Measurements were performed using 25 μM calmodulin at 20 °C in 10 mM Tris, 100 mM KCl, pH 8. Calibration with the indicator shows that the calmodulin is at least 99% calcium free at the start of the titration. The peptide to protein ratio was ≈4:1 for all experiments. At least four separate titrations were performed on each protein sample, and the values for the individual binding constants (K_1 to K_4) were obtained from least-squares fits directly to the experimentally observed titration curves (Linse et al., 1991a). Stock solutions of $CaCl_2$ were prepared by dilution of a volumetric standard and checked by titration with 5,5′-Br_2BAPTA.

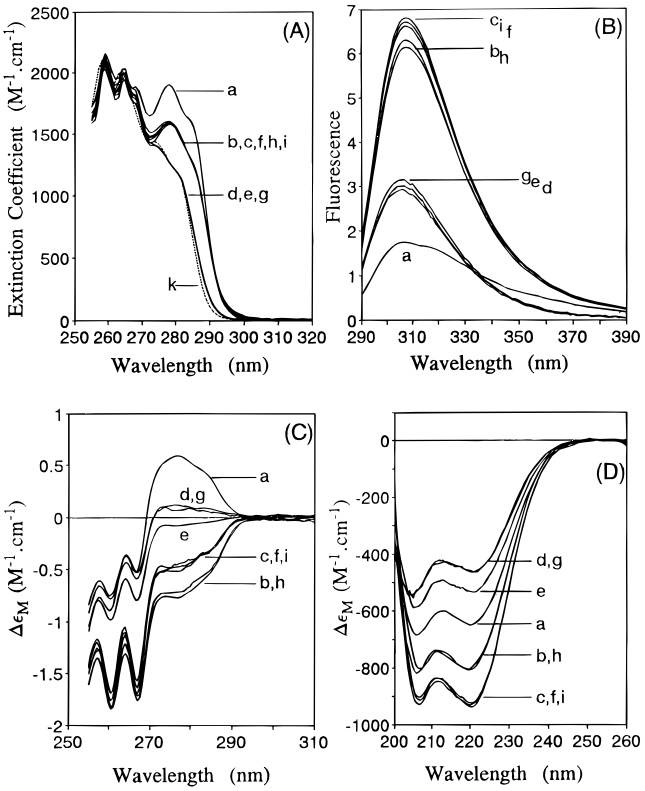

FIGURE 1: Optical spectra of calmodulin and calmodulin−peptide complexes: (A) absorption spectra; (B) fluorescence emission spectra; (C) near-UV CD spectra; (D) far-UV CD spectra. Wild-type: apo (a), holo (b), holo−peptide complex (c). V136G: apo (d), holo (e), holo−peptide complex (f). I100G: apo (g), holo (h), holo−peptide complex (i). The peptide used was CBP1, except for far-UV CD spectra where WFF was used. The dotted line (k) in panel (A) is the calculated absorption spectrum for a mixture of nine phenylalanines and one tyrosine. Note: For panel D, $\Delta\epsilon_{MRW}$ can be obtained by dividing $\Delta\epsilon_M$ by 147 (curves a, b, d, e, g, h) or 164 (curves c, f, i).

RESULTS

Absorption Spectroscopy. The absorption spectra of wild-type *Drosophila* CaM are shown in Figure 1A. There is a substantial Ca-induced *decrease* in the absorption of the single tyrosine (Y138) at 279 nm (ϵ_{279nm} = 1874 M^{-1} cm^{-1} for apo-CaM(WT), curve a, and 1578 M^{-1} cm^{-1} for Ca_4-CaM(WT), curve b; Maune et al., 1992a). The addition of 1 equiv of a spectroscopically "silent" peptide (FFF or CBP1) to Ca_4-CaM(WT) causes no change in the absorption spectrum (curve c). These spectra are much more intense than the spectrum of CaM(WT) in 6 M guanidine hydrochloride (Maune et al., 1992a), which is closely similar to the spectrum calculated for a 9:1 mole ratio mixture of Phe and Tyr (calculated ϵ_{280nm} = 1280 M^{-1} cm^{-1}; Gill and von Hippel, 1986). This calculated spectrum is the dotted line (curve k) in Figure 1A. The apo- and holo-forms of CaM-(I27G) and CaM(I63G) have spectra which are identical to those of the corresponding wild-type forms, and we have

therefore used the extinction coefficients of the wild-type in determining concentrations of these mutants.

The C-terminal mutants have very different properties. The spectra of the apo- and holo-forms of CaM(V136G) (curves d and e) are the same (i.e., there is no Ca-induced change for this mutant), and they are almost unchanged in 6 M GuHCl. The addition of 1 equiv of silent peptide (CBP1) to Ca_4-CaM(V136G) causes a large *increase* in Tyr absorption, and the spectrum of Ca_4-CaM(V136G)-CBP1 (curve f) is the same as that of Ca_4-CaM(WT) or Ca_4-CaM(WT)-CBP1 (curves b and c). The spectrum of apo-CaM(I100G) (curve g) is the same as that of apo-CaM(V136G) (curve d) and is also unchanged in 6 M GuHCl. The addition of calcium causes a substantial *increase* in tyrosine absorption, and the spectrum of Ca_4-CaM(I100G) (curve h) is the same as that of Ca_4-CaM(WT) (curve b). The addition of 1 equiv of silent peptide (CBP1) to Ca_4-CaM(I100G) causes no further changes. For these mutants, the calculated ϵ_{280nm} (1280 M^{-1} cm^{-1}) for a 9:1 mole ratio mixture of Phe and Tyr has been used in determining the concentration in the apo-form.

Fluorescence Spectroscopy. There is a large (≈3-fold) Ca-induced *increase* in the tyrosine emission intensity of wild-type *Drosophila* CaM (Figure 1B, curves a and b). The addition of 1 equiv of a silent peptide (FFF or CBP1) to Ca_4-CaM(WT) causes a small further increase in emission intensity (curve c). The shape of the apo-CaM(WT) emission spectrum differs significantly from that of simple model compounds such as *N*-acetyl tyrosine amide and the emission maxima for the three forms of the protein are at an unusually long wavelength for Tyr (307−308 nm for apo-CaM(WT), 308−309 nm for Ca_4-CaM(WT) and Ca_4-CaM(WT)-CBP1). Tyrosine emission spectra of the N-terminal β-sheet mutants CaM(I27G) and CaM(I63G) are identical to those of the corresponding forms of the wild-type.

The tyrosine emission spectra of the apo- and holo-forms of CaM(V136G) (curves d and e) are essentially the same (i.e., there is no Ca-induced change for this mutant), and the band shape and emission maxima (305−306 nm) are very similar to those of *N*-acetyl tyrosine amide. The addition of 1 equiv of a silent peptide (FFF or CBP1) to Ca_4-CaM-(V136G) causes a large *increase* in tyrosine emission intensity and a shift in the emission maximum to 308−309 nm. The spectrum of Ca_4-CaM(V136G)-CBP1 (curve f) is very similar to that of Ca_4-CaM(WT)-CBP1 (curve c). The apo-CaM(I100G) emission spectrum (curve g) is the same as that of apo-CaM(V136G) (curve d). The addition of calcium causes a substantial increase in tyrosine emission and a shift in the emission maximum to 308−309 nm; the spectrum of Ca_4-CaM(I100G) (curve h) is essentially the same as that of Ca_4-CaM(WT) (curve b). The addition of silent peptide (FFF or CBP1) to Ca_4-CaM(I100G) causes a small further increase (curve i), as with the wild-type.

Near-UV Circular Dichroism. For wild-type *Drosophila* CaM there is a major Ca-induced change in the CD signal from Y138 (Figure 1C; $\Delta\epsilon_{279nm} = 0.55$ M^{-1} cm^{-1} for apo-CaM(WT) (curve a) and -0.692 M^{-1} cm^{-1} for Ca_4-CaM-(WT) (curve b); Maune et al., 1992b). The addition of 1 equiv of silent peptide (FFF or CBP1) to Ca_4-CaM(WT) changes $\Delta\epsilon_{279nm}$ to ≈ -0.44 M^{-1} cm^{-1} (curve c). The spectra of the apo- and holo-forms of the CaM(I27G) and CaM-(I63G) are identical to those of the corresponding forms of the wild-type.

The spectrum of apo-CaM(V136G) (curve d) is much less intense than that of apo-CaM(WT) (curve a), and the addition of calcium produces only a small change (curve e). However, the addition of 1 equiv of silent peptide (FFF or CBP1) to Ca_4-CaM(V136G) causes a substantial change in the tyrosine CD, and the spectrum of Ca_4-CaM(V136G)-CBP1 (curve f) is the same as that of Ca_4-CaM-CBP1 (curve c). The spectrum of apo-CaM(I100G) (curve g) is the same as that of apo-CaM(V136G) (curve d). The addition of calcium causes a large change in the Tyr CD, and the Ca_4-CaM-(I100G) spectrum (curve h) is the same as that of Ca_4-CaM. The addition of 1 equiv of a silent peptide (CBP1) to form Ca_4-CaM(I100G)-CBP1 (curve i) reduces the tyrosine CD intensity, as with the wild-type protein.

Near-UV CD spectra of 1:1 complexes of Ca_4-CaM-(I100G) and Ca_4-CaM(V136G) with peptides WFF and FFW (not shown) are identical to those of the corresponding Ca_4-CaM(WT) complexes (Findlay et al., 1995a), suggesting that the peptides bind to the mutants and the wild-type in the same way (i.e., with W4 (WFF) or F4 (FFW) interacting with the C-terminal domain of CaM and F17 (WFF) or W17 (FFW) interacting with the N-terminal domain of CaM; Findlay et al., 1995a,b).

Far-UV Circular Dichroism. Figure 1D shows the far-UV CD spectra of wild-type *Drosophila* CaM in the apo-form (curve a) and holo-form (curve b). There is a large Ca-induced increase in intensity throughout the far-UV region which is associated with changes in the secondary structure of the calmodulin (Bayley and Martin, 1992; Maune et al., 1992b). The addition of 1 equiv of WFF peptide to Ca_4-CaM(WT) produces a further significant increase in CD intensity (curve c), consistent with the peptide, which is unstructured when free in solution, adopting a largely α-helical structure in Ca_4-CaM-WFF (Findlay et al., 1995a).

The spectrum of apo-CaM(V136G) (curve d) is much less intense than that of apo-CaM(WT) (curve a), and the addition of calcium produces only a small increase in intensity (curve e). However, the addition of 1 equiv of the WFF peptide to Ca_4-CaM(V136G) causes a very large increase in intensity so that the spectrum of Ca_4-CaM(V136G)-WFF (curve f) is the same as that of Ca_4-CaM(WT)-WFF (curve c). Effectively identical results were obtained when these measurements were repeated using the FFF peptide. The spectrum of apo-CaM(I100G) (curve g) is the same as that of apo-CaM(V136G) (curve d). In this case, the addition of calcium causes a very large increase in the CD intensity and the spectrum of Ca_4-CaM(I100G) (curve h) is the same as that of Ca_4-CaM(WT) (curve b). The addition of 1 equiv of WFF peptide to form Ca_4-CaM(I100G)-WFF (curve i) increases the intensity as with the wild-type protein.

The I27G and I63G mutants behave in a very similar way to the I100G mutant (not shown). Thus, the apo-forms have reduced far-UV CD intensity, similar to that of the apo-CaM-(I100G). The addition of calcium causes a large increase in the CD intensity, and the spectra of holo-forms are the same as that of Ca_4-CaM(WT). The addition of 1 equiv of WFF peptide increases the intensity as with the wild-type protein.

Thermal Unfolding. The changes in near-UV CD of the apo- and holo-forms of the wild-type protein at 279 nm as a function of temperature are shown in Figure 2. Measurements at this wavelength monitor changes in the environment of Y138 in the C-terminal domain of the CaM. In the absence of calcium the CD signal is lost in a single transition

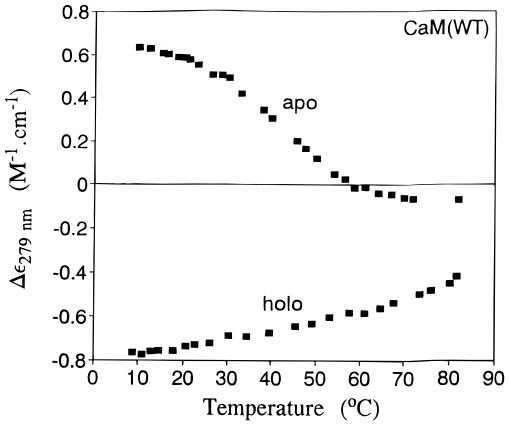

FIGURE 2: Near-UV CD thermal unfolding profiles for holo- and apo-wild-type *Drosophila* calmodulin. The buffer was 25 mM Tris, 100 mM KCl (pH 8.0) with 5 mM $CaCl_2$ or 1 mM EGTA as appropriate.

with an apparent midpoint of ≈42 °C. The breadth of the transition corresponds to an enthalpy of unfolding of ≈20 kcal/mol. In the presence of Ca the CD signal decreases monotonically by approximately 40% in the range 10−83 °C. (Kilhoffer et al. (1981) have reported a very similar curve for the unfolding of ram testis calmodulin, which contains Y99 in addition to Y138.) These results show that, in the presence of Ca, the C-terminal domain undergoes complete unfolding only at $T > 90$ °C.

Figure 3 shows the temperature dependence of the far-UV CD for wild-type *Drosophila* calmodulin and the I100G mutant. Figure 3A shows the behavior of Ca_4-CaM(WT) in aqueous buffer and in 2.5−12.5% (v/v) aqueous trifluoroethanol (TFE). Increasing temperature results in a steady decrease in the CD signal, but no major unfolding occurs in the temperature range studied. Low concentrations of TFE increase the intensity of the CD signal (cf. Bayley and Martin, 1992) without causing a major change in the form of the curve. Apo-CaM(WT) behaves very differently (Figure 3B). There is a broad transition between 30 and 70 °C which corresponds in amplitude to complete unfolding of the protein, as noted by Brzeska et al. (1983). In the interpretation of Tsalkova and Privalov (1985), this broad transition corresponds to overlapping transitions at 36 °C (C-domain) and 54 °C (N-domain). There is again a relatively small effect of TFE (0−12.5%) on the CD intensity at low temperatures but a larger effect at high temperatures, suggesting that TFE may have some stabilizing effect on the N-terminal domain.

Ca_4-CaM(I100G) has a fully folded C-terminal domain at room temperature (Figure 1D); far-UV CD thermal unfolding profiles are shown in Figure 3C. Increasing the temperature unfolds the C-terminal domain with a T_m of ≈50 °C, ($\Delta H \approx 30$ kcal/mol). The CD intensity then remains approximately constant up to 83 °C. Increasing [TFE] increases the thermal stability of the C-terminal domain so that the thermal unfolding profile at 12.5% TFE is closely similar to that for Ca_4-CaM(WT) in 12.5% TFE (compare curve f with the open squares in Figure 3C). Thermal unfolding profiles for apo-CaM(I100G), which has a partially folded C-terminal domain at room temperature (Figure 1D), are shown in Figure 3D. The residual C-domain structure is lost upon heating to $T \approx 25$ °C, and T_m is evidently close to 0 °C. Increasing [TFE] partially restores the secondary

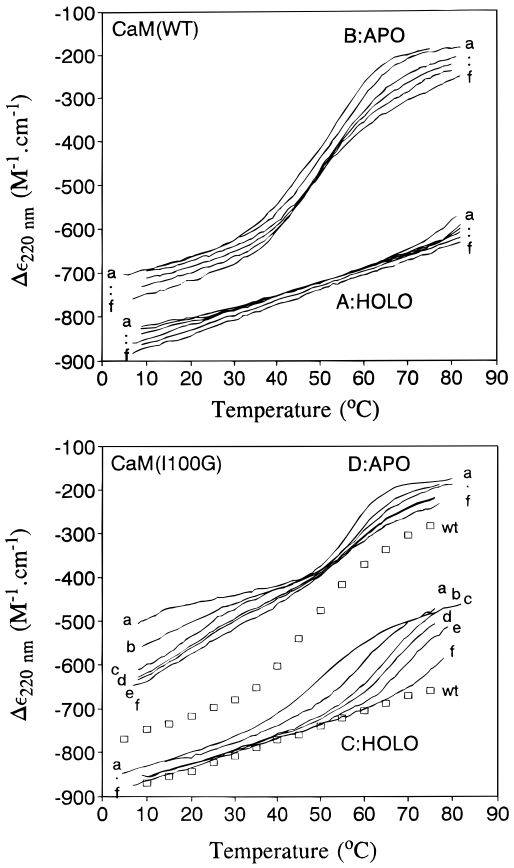

FIGURE 3: Far-UV CD thermal unfolding profiles for holo- and apo-wild-type CaM and holo- and apo-CaM(I100G) as a function of volume (%) TFE: (A) Ca_4-CaM in 0 (a), 2.5 (b), 5 (c), 7.5 (d), 10 (e), and 12.5% (f) TFE; (B) apo-CaM in 0 (a), 2.5 (b), 5 (c), 7.5 (d), 10 (e), and 12.5% (f) TFE; (C) Ca_4-CaM(I100G) in 0 (a), 2.5 (b), 5 (c), 7.5 (d), 10 (e), and 12.5% (f) TFE; (D) apo-CaM-(I100G) in 0 (a), 2.5 (b), 5 (c), 7.5 (d), 10 (e), and 12.5% (f) TFE. The open squares in panels C and D are the thermal unfolding curves for the holo- and apo-forms of the wild-type protein in 12.5% TFE (taken from panels A and B).

structure of the apo form of the C-terminal domain at low temperatures and increases its thermal stability.

Far-UV CD thermal unfolding profiles for the mutant Ca_4-CaM(V136G), which has a partially folded C-terminal domain at room temperature (Figure 1D), are shown in Figure 4A. Upon heating, the C-domain structure is lost by $T \approx 35$ °C (curve a), and the CD intensity then remains approximately constant up to 83 °C, indicating that there is no major unfolding of the N-terminal domain. The estimated T_m for the mutant C-domain is ∼0 °C, i.e., at least 80 °C less than the corresponding C-domain of Ca_4-CaM(WT). Increasing [TFE] has two effects: (1) The CD intensity recorded at low temperatures is dramatically increased, so that low concentrations of TFE (<12.5%) fully restore the secondary structure of the holo-form of the C-terminal domain of Ca_4-CaM(V136G). (2) The thermal stability of the mutant C-terminal domain is significantly increased by low concentrations of TFE (e.g., 2.5%, curve c in Figure 4A). The thermal unfolding profile in 12.5% TFE is closely similar to that for Ca_4-CaM in 12.5% TFE (compare curve g with the open squares in Figure 4A). Thus 12.5% TFE shifts the T_m for unfolding of the holo-form of the mutant C-domain by >80 °C.

Far-UV CD thermal unfolding profiles for apo-CaM-(V136G) are shown in Figure 4B. The C-domain structure

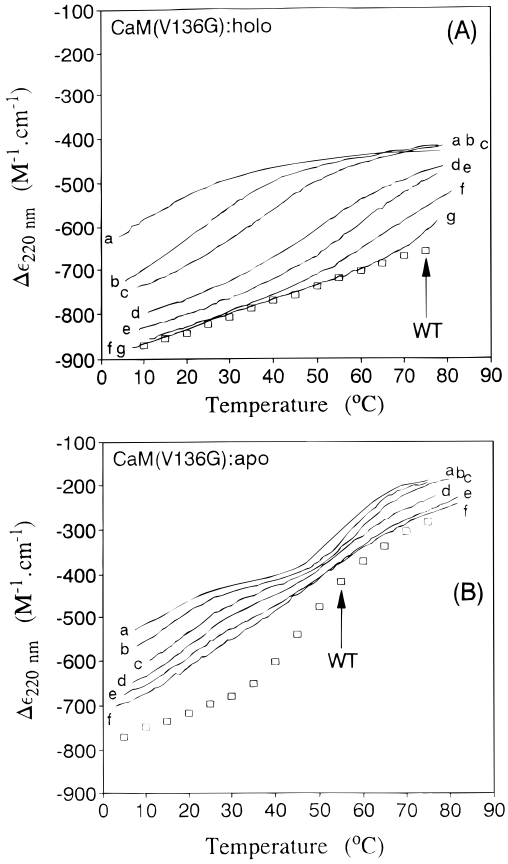

FIGURE 4: Far-UV CD thermal unfolding profiles for holo- and apo-CaM(V136G) as a function of volume (%) TFE: (A) Ca_4-CaM(V136G) in 0 (a), 1.25 (b), 2.5 (c), 3.75 (d), 5 (e), 10 (f), and 12.5% (g) TFE; (B) apo-CaM(V136G) in 0 (a), 2.5 (b), 5 (c), 7.5 (d), 10 (e), and 12.5% (f) TFE. The open squares in panels A and B are the thermal unfolding curves for the holo- and apo-forms of the wild-type protein in 12.5% TFE (taken from Figure 3).

is lost upon heating to $T \approx 30$ °C (see curve a). Major unfolding of the N-terminal domain then occurs with $T_m \approx 58$ °C ($\Delta H \approx 40$ kcal/mol). Again low concentrations of TFE largely restore the secondary structure of the apo-form of the mutant C-domain at low temperatures and increase its thermal stability, albeit to a lesser extent than for Ca_4-CaM(V136G) (compare curve f with the open squares in Figure 4B).

Figure 5 shows far-UV CD thermal unfolding profiles for the apo- and holo-forms of the mutants CaM(I27G) and CaM(I63G) in aqueous buffer. The two proteins behave in a way consistent with the mutation reducing the stability of the N-terminal domain. The N-terminal domains of the holo-forms are fully folded at $T < 20$ °C but unfold in a broad transition at $T_m \approx 35-40$ °C ($\Delta H \approx 25$ kcal/mol). Unfolding of the holo C-terminal domain occurs only at $T > 80$ °C. The N-terminal domains of the apo-forms of these mutants are at least partially unfolded at $T \approx 10$ °C, and the unfolding occurs with $T_m < 20$ °C, compared with $T_m \approx 55$ °C for the nonmutated N-terminal domain. Although not fully resolved, a second transition evidently occurs at $T_m > 40$ °C, consistent with the unfolding of the C-terminal domain. The near-UV CD thermal unfolding profile for apo-CaM(I27G) (not shown) is very similar to that for the wild-type protein (Figure 2), showing that the mutation in the N-terminal domain does not affect the thermal stability of the C-terminal domain. The parameters for all the thermal transitions are

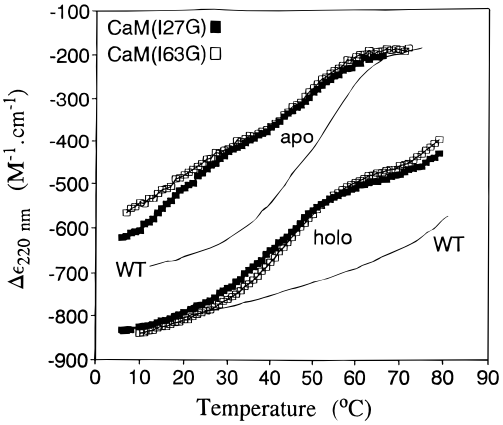

FIGURE 5: Thermal unfolding profiles for CaM(I27G) and CaM(I63G): (A) far-UV CD unfolding profiles for apo- and holo-CaM(I27G) (■) and CaM(I63G) (□); (B) near-UV CD unfolding profile for apo-CaM(I27G).

given in Table 3; these are generally only approximate values owing to the sloping background of the thermal profile and the presence of overlapping transitions. More precise values are presently being sought by calorimetric methods.

Peptide Affinities. The affinities of wild-type *Drosophila* calmodulin and the four β-sheet mutants for three tryptophan-containing peptides (WFF, FFW, and FWF; see Materials and Methods) were measured by direct fluorometric titration at 20 °C (titration data not shown). The results (summarized in Table 1) show that, for the three peptides examined, the affinity for the mutant protein is always lower than for the wild-type protein.

For Ca_4-CaM(V136G) the affinities are 72, 10.5, and 20.9 times lower for WFF, FWF, and FFW, respectively. For Ca_4-CaM(I100G) the affinities are 8.5, 2.7, and 6.1 times lower for WFF, FWF, and FFW, respectively. Thus, the two C-terminal mutant proteins show a somewhat similar pattern of behavior with the three peptides, with the V136G mutation always having a slightly more deleterious effect on the strength of peptide binding. For both mutants the effect of the mutation is greatest for the WFF peptide and smallest for the FWF peptide. The maximum fluorescence enhancement observed on binding the peptide is generally somewhat lower with the mutant proteins, especially for the WFF peptide.

For Ca_4-CaM(I27G) the affinities are 7.7, 5.7, and 47.2 times lower for WFF, FWF, and FFW peptides, respectively. For Ca_4-CaM(I63G) the affinities are 3.6, 2.2, and 21.7 times lower for WFF, FWF, and FFW peptides, respectively. Thus, the two N-terminal mutant proteins also show a similar pattern of behavior with the three peptides; in this case, the I27G mutation always has a slightly more deleterious effect on peptide affinity. The pattern of behavior with the three peptides is significantly different from that shown by the two C-terminal mutants. As with the C-terminal mutants, the effect is smallest for the FWF peptide, but in this case the greatest effect is observed for the FFW peptide.

Calcium Binding. The indicator method (Linse et al., 1988, 1991a; Martin et al., 1996; Bayley et al., 1996) has been used to determine the stoichiometric calcium binding constants for the four β-sheet mutants in the presence and absence of the WFF peptide. Typical experimental data for calcium titrations of 5,5′-Br_2BAPTA in the presence of wild-type *Drosophila* calmodulin and the two C-terminal mutants

Table 1: Affinities of Wild-Type *Drosophila* Calmodulin and the Four β-Sheet Mutants for Three Tryptophan-Containing Peptides[a]

	K_d (nM) [F_{Pp}/F_p][b]				
peptide	wild-type	CaM(I27G)	CaM(I63G)	CaM(I100G)	CaM(V136G)
WFF	0.145 (0.04)[c]	1.12 (0.21)	0.53 (0.18)	1.22 (0.31)	10.45 (2.5)
	[2.75 (0.05)]	[2.52 (0.02)]	[2.63 (0.03)]	[2.29 (0.06)]	[2.05 (0.05)]
FWF	6.2 (1.15)	35.2 (4.5)	13.2 (5.1)	17.0 (4.0)	64.4 (13)
	[2.60 (0.05)]	[2.42 (0.06)]	[2.63 (0.03)]	[2.29 (0.04)]	[2.11 (0.05)]
FFW	1.77 (0.35)[c]	83.5 (12.7)	38.5 (5.6)	12.5 (3.5)	37.0 (4.0)
	[2.90 (0.05)]	[2.34 (0.04)]	[2.48 (0.06)]	[2.70 (0.06)]	[2.70 (0.05)]

[a] The measurements were made at 20 °C in 25 mM Tris, 100 mM KCl, 1 mM $CaCl_2$ at pH 8. The values in parentheses are standard deviations. [b] F_{Pp}/F_p is the fluorescence enhancement at the wavelength of measurement (generally 332 or 334 nm). [c] Determined by competition with a spectroscopically silent peptide (CBP1) of known affinity (S. R. Martin and P. M. Bayley, manuscript in preparation).

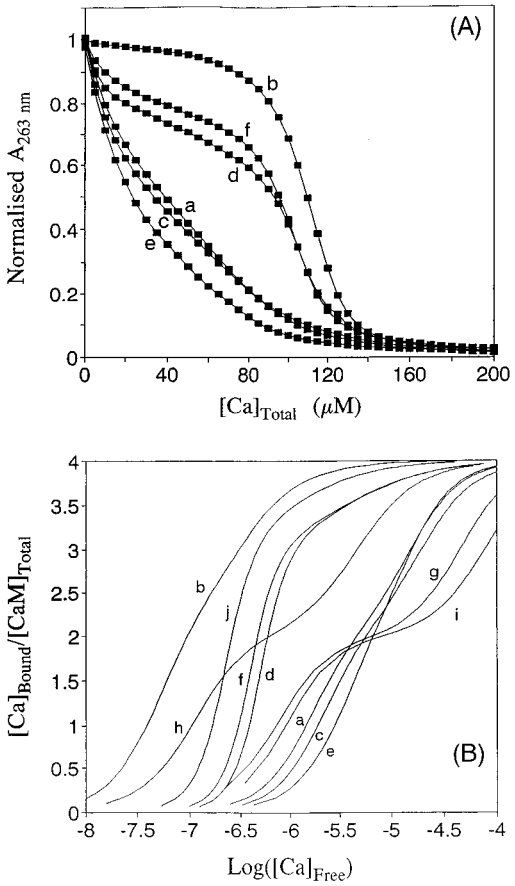

FIGURE 6: Calcium binding to calmodulin and calmodulin mutants. (A) Typical experimental data for calcium titrations of 5,5′-Br_2-BAPTA (25 μM) in the presence of CaM (a), CaM plus WFF peptide (b), CaM(V136G) (c), CaM(V136G) plus WFF peptide (d), CaM(I100G) (e), and CaM(I100G) plus WFF peptide (f). The protein concentration was 25 μM and the [WFF] to [protein] ratio was ≈4:1. The curves through the points are the least-squares fits to the data. The error on individual points is less than the size of the symbols. The total absorbance change has been normalized in order to facilitate comparison. Note: The curve for CaM plus WFF peptide is for illustrative purposes only. The K_i values for this system were determined in titrations using Quin 2 (Martin et al., 1996). (B) Calcium binding to CaM (a), CaM in the presence of WFF peptide (b), CaM(V136G) (c), CaM(V136G) plus WFF peptide (d), CaM(I100G) (e), CaM(I100G) plus WFF peptide (f), CaM(I27G) (g), CaM(I27G) plus WFF peptide (h), CaM(I63G) (i), and CaM(I63G) plus WFF peptide (j). The calcium binding profiles were calculated from the stoichiometric binding constants determined from calcium titrations in the presence of 5,5′-Br_2BAPTA or Quin 2 (see part A and Table 2).

are shown in Figure 6A. The stoichiometric association constants obtained from the analysis of such experiments are listed in Table 2. These constants were used to calculate curves for the variation of the degree of saturation of the different calmodulins with calcium as a function of log-($[Ca]_{free}$), and these are shown in Figure 6B.

It is evident from Figure 6B and Table 2 that two distinct patterns of calcium binding are observed in the absence of added peptide. For the C-terminal mutants, the effect of the mutation is to reduce log(K_1K_2) slightly while leaving log-(K_3K_4) largely unaffected. The wild-type protein and the two C-terminal mutants therefore show a very similar pattern of calcium binding (curves a, c, and e in Figure 6B). For the two N-terminal mutants the effect of the mutation is to *increase* log(K_1K_2) slightly and to reduce log(K_3K_4) significantly. Consequently, the calcium saturation curves for these mutants are biphasic (curves g and i in Figure 6B), and they are therefore quite distinct from those of the other three proteins.

All the proteins examined bind calcium much more strongly in the presence of the WFF peptide, but the effect of the peptide on the calcium affinity of the mutant proteins is substantially less than on the wild-type. For the wild-type protein both log(K_1K_2) and log(K_3K_4) are significantly higher in the presence of peptide (by 3.05 and 3.45 log units, respectively). For the C-terminal mutants and the I63G mutant there is little effect of peptide on log(K_1K_2), but log-(K_3K_4) is increased by between 3.5 and 5.2 log units. For all three proteins this increase in log(K_3K_4) is largely due to a major increase in K_3. The calcium saturation behavior is therefore very similar for these three mutants (curves d, f, and j in Figure 6B). In contrast, for the I27G mutant both log(K_1K_2) and log(K_3K_4) are increased in the presence of peptide but only by 1.65 and 2 log units, respectively. The calcium saturation behavior of this mutant is biphasic (curve h in Figure 6B) and is very different from those of the other four proteins.

Figure 6 illustrates the inter-relationship of the calcium affinity of calmodulin itself and the calcium-dependent increase in peptide affinity for calmodulin. As shown elsewhere (Yazawa et al., 1992; Bayley et al., 1996) the calcium-induced increase in the affinity of CaM for a particular peptide (K_d/K'_d, where K_d and K'_d are the dissociation constants for peptide binding in the presence and absence of calcium) may be estimated from the stoichiometric calcium binding constants measured for calmodulin alone ($K_1...K_4$) and for calmodulin in the presence of excess peptide ($K'_1...K'_4$) through the equation:

$$K'_d/K_d = (K'_1K'_2K'_3K'_4)/(K_1K_2K_3K_4)$$

The use of this equation assumes that the stoichiometric association constants measured in the presence of excess peptide (K'_1 to K'_4) are the true values of these constants. In

Table 2: Macroscopic Ca^{2+} Binding Constants for Calmodulin and the Four β-Sheet Mutants in the Presence and Absence of the WFF Peptide[a]

sample	log(K_1)	log(K_2)	log(K_3)	log(K_4)	log(K_1K_2)	log(K_3K_4)
Drosophila CaM[b]	5.23 (0.14)	6.42 (0.20)	4.33 (0.31)	5.33 (0.20)	11.65 (0.15)	9.66 (0.25)
Drosophila CaM + WFF[b]	6.79 (0.23)	7.91 (0.25)	6.57 (0.24)	6.53 (0.21)	14.70 (0.16)	13.10 (0.17)
CaM(I27G)	5.83 (0.12)	6.46 (0.11)	3.77 (0.21)	4.93 (0.15)	12.29 (0.13)	8.70 (0.11)
CaM(I27G) + WFF	6.60 (0.18)	7.35 (0.17)	5.22 (0.19)	5.45 (0.17)	13.95 (0.09)	10.67 (0.12)
CaM(I63G)	5.55 (0.12)	6.54 (0.13)	3.69 (0.11)	4.54 (0.16)	12.10 (0.04)	8.23 (0.31)
CaM(I63G) + WFF	5.64 (0.13)	6.84 (0.18)	7.42 (0.11)	6.03 (0.23)	12.48 (0.18)	13.45 (0.08)
CaM(I100G)	5.06 (0.14)	5.97 (0.13)	4.25 (0.16)	5.45 (0.18)	11.03 (0.08)	9.70 (0.09)
CaM(I100G) + WFF	5.18 (0.18)	6.37 (0.27)	7.65 (0.18)	5.46 (0.15)	11.55 (0.09)	13.11 (0.12)
CaM(V136G)	5.06 (0.21)	6.34 (0.17)	4.38 (0.23)	5.08 (0.19)	11.40 (0.15)	9.46 (0.08)
CaM(V136G) + WFF	5.08 (0.19)	6.29 (0.17)	7.50 (0.18)	5.45 (0.21)	11.37 (0.13)	12.95 (0.11)

[a] Measurements were made at 20 °C in 10 mM Tris, 100 mM KCl, pH 8.0. The values in parentheses are the standard deviations. [b] These values are from Martin et al. (1996).

Table 3: Thermodynamic Parameters for the Thermal Transitions

	apo-form				holo-form			
	N-domain		C-domain		N-domain		C-domain	
protein	T_m (°C)	ΔH (kcal/mol)	T_m (°C)	ΔH (kcal/mol)	T_m (°C)	ΔH (kcal/mol)	T_m (°C)	ΔH (kcal/ol)
wild-type	*b*	nd	42[c]	20	>80	nd	>80	nd
wild-type[f]	55	nd	30	nd	>90	nd	>90	nd
wild-type[g]	54	48	36	27	>115[d]	nd	>115	nd
					>101[e]	nd	85	nd
V136G	55	40	≈0	(20)	>80	nd	≈0	(13)
V136G (12.5% TFE)	*b*	nd	*b*	nd	>80	nd	>80	(46)
I100G	55	40	≈0	(20)	>80	nd	50	30
I100G (12.5% TFE)	*b*	nd	*b*	nd	>80	nd	>80	(40)
I63G	<20	nd	*b*	nd	40	(40)	>80	nd
I27G	<20	nd	42[c]	20	35	25	>80	nd

[a] nd = not determined. Parentheses indicate approximate values. [b] Transition present but not resolved. [c] Near-UV CD data. [d] [Ca] ≈ 10^{-5} M. [e] [Ca] estimated as ≈10^{-7} M; the presence of a peak at 49 °C might indicate incomplete Ca saturation. [f] From Brzeska et al. (1983). [g] From Tsalkova and Privalov (1985).

fact, the true values will only be measured under conditions where the protein can be totally saturated with peptide in the *absence* of calcium. This is not generally achievable experimentally since the affinity of the peptide for the protein in the absence of Ca is usually low. The measured values will, in general, be less than the true ones, and the calculated value of K'_d/K_d will therefore be only a lower estimate. Values of K'_d calculated from data such as that given in Tables 1 and 2 will therefore tend to be underestimates. The values calculated for K'_d (for peptide WFF) are therefore ≥450 μM (CaM), ≥5 μM (CaM(I27G)), ≥200 μM (CaM(I63G)), ≥10 μM (CaM(I100G)), and ≥30 μM (CaM(V136G)), suggesting that mutation of either domain may well increase the interaction of the apo-calmodulin species with a target sequence.

Stopped-Flow Studies. The kinetics of calcium dissociation from *Drosophila* calmodulin, the two C-terminal β-sheet mutants, and the I63G N-terminal mutant have been measured, and typical experimental curves are shown in Figure 7. Under the conditions used we do not see dissociation from the N-terminal sites because the dissociation rate constant is greater than 850 s^{-1} (Brown et al., 1997) and dissociation is therefore expected to be >95% complete within the deadtime of the instrument (estimated at 3−4 ms).

Figure 7 shows that the dissociation of two Ca ions occurs with rates 7.9 ± 0.5, 36.5 ± 0.5, and 92.5 ± 11.5 s^{-1} for the WT, V136G, and I100G calmodulin species respectively; a value of 6.5 ± 1.2 s^{-1} was obtained for I63G (not shown). In agreement with previous studies, this rate corresponds to the dissociation from the C-domain. Mutation of either V136G or I100G increases the rate, consistent with the decreased Ca affinity seen in Table 2 and Figure 7. The N-domain mutation I63G has no significant effect on the Ca dissociation from the C-domain.

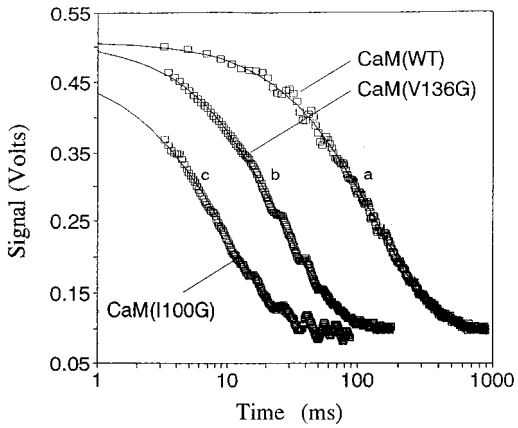

FIGURE 7: Calcium dissociation from calmodulin and calmodulin mutants. Typical experimental stopped-flow data for the Quin 2-induced dissociation of calcium from wild-type *Drosophila* calmodulin and the two mutants. The rates and amplitudes calculated for the fitted curves were 7.3 s^{-1} and 0.40 V (Ca_4-CaM(WT)), 103 s^{-1} and 0.37 V (Ca_4-CaM(I100G)), and 38 s^{-1} and 0.41 V (Ca_4-CaM(V136G)). A decrease of 0.4 V corresponds to an increase in fluorescence equivalent to dissociation of two calcium ions.

DISCUSSION

Optical Spectroscopy. The absorption spectra of wild-type *Drosophila* CaM, which contains a single Tyr residue at position 138, have been well characterized (Maune et al.,

1992a). The Tyr absorption of apo-CaM at 280 nm is ≈47% more intense than expected for a 9:1 mole ratio mixture of Phe and Tyr. The extinction coefficient of the Tyr in the apo-protein is considerably higher even than that of tyrosine model compounds in propanol (Pace et al., 1995), suggesting that this residue is in an unusual environment. The addition of calcium causes a decrease in Tyr absorption, but ϵ_{280nm} remains ≈23% higher than the calculated value. The formation of a complex between Ca_4-CaM(WT) and a silent peptide (FFF or CBP1) does not cause any significant change in the Tyr absorption, although it does affect the Tyr fluorescence and near-UV CD properties (see below). In the crystal structure of Ca_4-CaM(WT) the phenolic OH of Tyr-138 is apparently hydrogen bonded to Glu-82 (Babu et al., 1988), suggesting a possible cause for the spectroscopic perturbation. It is possible that the greater flexibility of the C-terminal domain in apo-CaM(WT) allows an enhanced interaction giving rise to the anomalously high UV absorbance.

The apo- and holo-forms of the N-terminal domain mutants (CaM(I27G) and CaM(I63G)) have absorption spectra which are essentially indistinguishable from the corresponding forms of the wild-type protein. In contrast, the absorption spectra of the apo-forms of the two C-terminal mutants are closely similar to the spectrum observed for a 9:1 mole ratio mixture of Phe and Tyr, suggesting that unlike wild-type CaM, Y138 is relatively solvent exposed in the apo-forms of these two proteins. In the case of CaM(V136G) there is little Ca-induced change in tyrosine absorption, but the addition of a silent peptide to Ca_4-CaM(V136G) produces a spectrum indistinguishable from that characteristic of Ca_4-CaM(WT) (and Ca_4-CaM(WT)-peptide). The addition of calcium to apo-CaM(I100G) is sufficient to produce the spectrum characteristic of Ca_4-CaM(WT) (and Ca_4-CaM-(WT)-peptide). The addition of the silent peptide causes no further change, as with the wild-type protein.

The near-UV CD and fluorescence experiments show the same pattern of behavior. For the wild-type protein the addition of calcium to the apo-form produces substantial changes in both Tyr emission and near-UV CD intensity. Small further changes are induced by the addition of silent peptide. The apo- and holo-forms of the N-terminal mutants have spectra which are indistinguishable from those of the corresponding forms of the wild-type, and addition of silent peptide produces similar effects. The spectra of the apo-forms of the C-terminal mutants are very different from the corresponding spectra of apo-CaM. The spectrum characteristic of Ca_4-CaM(WT) is produced by the addition of calcium to apo-CaM(I100G) but not to apo-CaM(V136G). For both mutants the addition of calcium *and* the silent peptide produces the spectrum characteristic of Ca_4-CaM-(WT)-peptide. The contribution of Y138 to the near-UV CD spectra of the apo-forms of the C-terminal mutant proteins is very weak, suggesting that this residue is mobile. The Tyr fluorescence emission spectra of these mutants have the same band shape and emission maximum as tyrosine model compounds, whereas apo-CaM(WT) has an unusually broad emission spectrum with an uncharacteristically long emission wavelength. This is further evidence for the unusual environment of this residue in the wild-type protein.

The far-UV CD spectrum is a sensitive indicator of α-helical secondary structure. Apo-CaM(V136G) is substantially less structured than apo-CaM(WT), and there is only a small Ca-induced increase in helicity. The addition of WFF (or similar target sequences) causes a large increase in helicity so that the spectrum of Ca_4-CaM(V136G)-WFF is effectively identical to that of Ca_4-CaM(WT)-WFF. The other three mutants behave in a different way. The apo-forms are much less structured than the wild-type (and are similar to apo-CaM(V136G)), but the addition of calcium is sufficient to produce the characteristic wild-type spectrum. Using the normal quantitation, we conclude that the apo-forms of all four mutants (and Ca_4-CaM(V136G)) contain 15−20 fewer helical residues than apo-CaM(WT), implying that, at 20 °C, the mutated apo N-domain lacks approximately one-half and the mutated apo C-domain three-fourths of the domain α-helical structure identified in the crystal and NMR structures of Ca_4-CaM(WT).

Thermal Unfolding. Previous studies on the thermal stability of calmodulin have shown that the holo-forms of the intact protein (and the tryptic fragments TR1C and TR2C) are extremely stable, with no major transitions observed at temperatures below 90 °C (Brzeska et al., 1983; Tsalkova and Privalov, 1985). The apo-forms of these proteins are very much less stable. Brzeska et al. (1983) showed that the first derivative of the far-UV CD thermal unfolding profile of apo-CaM exhibited a maximum at 55 °C and a shoulder at ≈30 °C. Using calorimetric methods, Tsalkova and Privalov (1985) resolved transitions at 36 and 54 °C, with $\Delta H = 27$ and 48 kcal/mol, respectively. The near-UV CD data (Figure 2) show $T_m \approx 42$ °C and $\Delta H \approx 20$ kcal/mol, identifying the apo C-domain as the less stable structure.

The thermal profiles of the mutants clearly show that for the apo-forms the domain containing the mutation is only partially folded at $T = 20$ °C and this residual structure is lost upon heating to 30−35 °C in all cases. Although the full amplitude of the transition is not always observable, the thermal transition of individual domains appears to conform to a two-state model of folded ↔ unfolded forms. Hence the loss of secondary structure in the mutants at $T = 20$ °C is interpreted as a decrease of T_m upon introduction of the mutation. We estimate that the T_m for unfolding of the mutated C- and N-domains is ≈0 and <20 °C for all the mutant calmodulins (cf. ≈42 and ≈ 55 °C for unfolding of the C- and N-terminal wild-type domains). Although the low-temperature limit cannot be reached, the folded form of the apo-mutant domain appears to be closely similar in secondary structure to that of the wild-type.

For the holo-forms the mutated domain is fully folded at $T = 20$ °C in all cases except the V136G mutant. In all cases the mutated domain has much lower thermal stability than in the wild-type protein. We estimate T_m values of approximately 0 and 48 °C for unfolding of the C-terminal domain in Ca_4-CaM(V136G) and Ca_4-CaM(I100G), respectively (cf. >85 °C for the C-terminal domain in Ca_4-CaM-(WT)), and 35−40 °C for unfolding of the N-terminal domains of Ca_4-CaM(I27G) and Ca_4-CaM(I63G) (cf. >85 °C for the N-terminal domain of Ca_4-CaM(WT)).

These results represent a truly remarkable perturbation of the T_m for individual calmodulin domains, caused by the introduction of a specific mutation of the hydrophobic residues involved in β-structure. Studies by Smith et al. (1994) and Smith and Regan (1995) have ranked the effectiveness of different amino acid side chains in antiparallel β-sheet conformations and placed Ile and Val among the most stable, correlating with their observed frequencies

of occurrence in β-sheets of known structure. In calmodulin, these residues contribute to the hydrophobic core; however, the mutation of the (non-β-sheet) residue Phe-92 (which is in close contact with Ile-100) in the calmodulin mutant F92A (Meyer et al., 1996) caused an apparent decrease in the T_m of apo-CaM by 12 °C (though unfolding of the two domains was not resolved). In the presence of calcium little effect of this mutation on unfolding was observed. By contrast, in the cases of the mutant apo N- and C-domains studied here, T_m is reduced by ≈40 °C, and for the C-domain in CaM(V_{136}G), ΔT_m exceeds 80 °C. The high thermal stability of several small proteins has been noted and rationalized by Alexander et al. (1992). Using the recent compilation of thermodynamic data of Myers et al. (1995), we take a value of $\Delta C_p \sim 14.2$ cal/(residue deg) which gives $\Delta C_p \approx 1$ kcal/(mol deg) for either calmodulin domain ($n \approx 75$). Taking the calorimetric and spectroscopic values of $\Delta H = 20-27$ kcal/mol for the unfolding of WT C-domain, and using the formulation of Schellman (1987) for the temperature dependence of the free energy of the domain, it can be seen that $\Delta\Delta G$ for the destabilization of a mutant domain by 1−2 kcal/mol can cause a change in T_m of approximately 40 °C (from 50 to 10 °C). The reason for the sensitivity of T_m in this case is the relatively low value of ΔH for unfolding the WT C-domain. For other well-studied proteins with $\Delta H > 100$ kcal/mol and ΔC_p of 1−2 kcal/(mol deg), a single mutation causing such a $\Delta\Delta G$ corresponds to a ΔT_m of only a few degrees Celcius (see Becktel and Schellman (1987) and Sturtevant (1993) for review).

An additional indication of the relatively small energies required to perturb the T_m of the mutants is the unusual sensitivity of the structure of the unfolded mutant domains in both apo- and holo-forms to low concentrations of the helicogenic solvent trifluoroethanol. In the case of the apo-proteins, although secondary structure is restored, the thermal stability is generally less than that of WT. In the case of the holo-proteins, the thermal stability of both the C-domain mutants is effectively fully restored. Thus TFE acts as a renaturant, and this effect may be due to increased stability of helical structures in the folded proteins (both apo and holo) as well as changes in the balance of solvation energies of folded and unfolded forms, compared to purely aqueous conditions. It is also notable that the binding of the target peptide WFF largely restores the thermal stability to the Ca_4-CaM(V136G) mutant (data not shown), and this can be seen as a positive shift in the energy surface on specific ligand binding, as described by Schellman (1987).

The effect on T_m of specific mutational substitutions in proteins of known structure is a powerful method of investigating the basis of thermodynamic stability of proteins, which has illuminated the important role of hydrophobic residues in forming a well-packed internal core structure (Richards and Lim, 1993). Different proteins show different capacity to tolerate hydrophobic substitutions and retain biological activity (Axe et al. (1996) and references therein). The example of the calmodulin domains appears unusual, in that the thermal stability of a domain is strongly reduced by the mutation but the conformational deficiency seen under normal temperatures is readily restored by the binding of Ca ion and an appropriate target sequence. Replacing a bulky hydrophobic group such as Ile or Val by Gly is expected to reduce the stability of the hydrophobic core in the folded form and also to introduce additional conformational entropy in the unfolded state. While both of these effects may be quite small, given the apparent flatness of the energy surface, these mechanisms appear adequate to explain the unusually large effects on T_m of the glycine mutations. In terms of biological function, the retention of essentially native WT structure in the holo-forms of the mutants suggests a reason for the strong conservation of each of the β-structure residues selected for mutation in this work. The apo-forms of all these mutant domains are effectively fully unfolded at physiological temperatures, presumably rendering such mutant calmodulins even more vulnerable to proteolytic cleavage in the apo-form and hence causing loss of function. The conservation of the β-structure between adjacent sites persists in the apo-form of wild-type calmodulin; this is evidently an important stabilizing feature in both the N- and C-domains, as well as its potential structural role in contributing to the Ca binding properties of each pair of EF-hands within either domain.

Peptide Affinities. The three peptides studied are derived from the M13 peptide, the 26-residue calmodulin target sequence of sk-MLCK. The WFF peptide is the first 18 residues of M13; FWF is WFF with W4F and F8W mutations, and FFW is WFF with W4F and F17W mutations. The residues in positions 4 and 17 are the important hydrophobic anchors for interaction with the calmodulin. All three peptides bind in the same orientation with the N-terminal portion of the peptide interacting with the C-terminal portion of the protein (Findlay et al., 1995b). The mutant proteins all bind the peptides with significantly lower affinity than the wild-type. For the C-terminal mutants the largest reduction in affinity compared with the wild-type occurs for the WFF peptide; for the N-terminal mutant the largest reduction is observed with the FFW peptide (see Table 1). Since the residue at position 4 in the peptide interacts with the C-terminal domain of CaM, while that at position 17 interacts with the N-terminal domain, these results confirm that the peptides bind with the expected polarity to the mutant calmodulins and that the Trp residue is important energetically in these interactions (cf. Findlay et al., 1995a).

The affinities of the peptides for Ca_4-CaM(V136G) are surprisingly high in view of the observation that the C-terminal domain of this mutant is only partially folded in the presence of calcium but that the binding of peptide restores the fully folded conformation of the C-terminal domain. Two possible reaction mechanisms can be distinguished. The first is that the peptide binds to the partially folded form and induces the re-folding of the C-terminal domain:

$$\text{Ca-CaM*} + \text{Pep} \leftrightarrow \text{Ca-CaM*-Pep} \leftrightarrow \text{Ca-CaM-Pep}$$

where CaM represents normally folded calmodulin, CaM* is calmodulin with a partially folded C-terminal domain, and Pep represents peptide. The second possible mechanism is that the peptide "selects" folded forms of the protein according to the following reaction:

$$\text{Ca-CaM*} \leftrightarrow \text{Ca-CaM} + \text{Pep} \leftrightarrow \text{Ca-CaM-Pep}$$

In either case, the relatively small effect of the mutation on peptide affinity in the presence of calcium appears consistent with a relatively small $\Delta\Delta G$ for the destabilization by mutation.

Equilibrium and Kinetic Studies of Calcium Binding. Following previous analyses (Bayley et al., 1996; Martin et al., 1996) we examined the products of the stoichiometric binding constants (i.e., K_1K_2 and K_3K_4) for the mutants. In the absence of peptide the calcium saturation behavior of the two C-terminal mutants is similar to that of the wild-type protein. Either mutation results in only a slight reduction in $\log(K_1K_2)$, with no change in $\log(K_3K_4)$. The calcium saturation behavior of the N-terminal mutants is very different with a biphasic appearance (see Figure 6B). This is because the mutations produce a slight increase in $\log(K_1K_2)$ and a large reduction in $\log(K_3K_4)$.

On the basis of studies with the separate N- and C-domains of wild-type CaM, it has been suggested (Linse et al., 1991a) that K_1 and K_2 reflect mainly the affinities of the two C-terminal sites, while K_3 and K_4 reflect mainly the affinities of the N-terminal sites. Consistent with this view the N-terminal mutations result in a large reduction in $\log(K_3K_4)$. The increase in $\log(K_1K_2)$ for these mutations is more difficult to rationalize since it suggests that the N-terminal mutation appears to increase the affinity of the C-terminal sites for calcium. The fact that $\log(K_3K_4)$ is unaffected by the C-terminal mutations is consistent with the view that these constants reflect the affinities of the N-terminal sites. However, the reduction in $\log(K_1K_2)$ for the C-terminal mutants is much less than the reduction in $\log(K_3K_4)$ for the N-terminal mutants (maximally 0.6 log unit for CaM-(I100G)). This is surprising in light of the spectroscopic observations showing that the C-terminal domain is even more unfolded in the apo state of the C-terminal mutants (compared to the N-terminal domain mutants). This might have been expected to reduce the overall calcium affinity owing to the free energy requirement to reform the "normal" conformation of the C-domain on binding calcium (for CaM-(I100G)). We note, however, that high calcium affinity (as shown by EF-hand proteins) is not necessarily dependent upon the "classical" helix−loop−helix conformation. For example, a 34 residue peptide derived from troponin C is able to bind calcium with high affinity even though it has a much lower helical content than the corresponding sequence in the full length protein (Reid et al., 1981). Furthermore, the calcium affinity is only slightly increased when the helical content of the peptide is increased by the addition of a helicogenic solvent (Reid et al., 1981). In fact the presence of Ca does not markedly affect the T_m for the unfolding of the V136G mutant domain. This suggests relatively strong binding of Ca to the unfolded form.

In the presence of the WFF peptide the values of $\log(K_1K_2)$ and $\log(K_3K_4)$ for the wild-type protein are increased by more than 3 log units (see Table 2), but since $\log(K_1K_2)$ remains considerably greater than $\log(K_3K_4)$, we deduce that intermediate calmodulin−peptide species can be formed with fewer than four calcium ions bound (cf. Bayley et al., 1996). The situation is rather similar for the I27G mutant, although the individual increases with peptide are significantly lower (1.6 and 2 log units for K_1K_2 and K_3K_4). Because $\log(K_1K_2)$ and $\log(K_3K_4)$ are increased by similar factors, the biphasic saturation behavior persists in the presence of the target peptide. For the other three mutants the situation is completely different. In the presence of the peptide the value of $\log(K_1K_2)$ is essentially unchanged but there is a major increase in $\log(K_3K_4)$, which is largely attributable to an increase in K_3. In this case the saturation curves suggest a more cooperative calcium binding behavior with less distinction between the properties of the two domains.

In summary, these results illustrate how changes in the properties of the calmodulin species can influence the calcium binding properties in both the absence and presence of a target sequence. In this case the changes were induced by a series of homologous replacements, but changes induced by natural sequence variation or by a change such as post-translational modification could presumably be equally effective. Since the calcium-dependent regulation of the calmodulin−target interaction derives from the difference in the two Ca saturation curves (for calmodulin ± peptide), it is clear that a wide diversity of both equilibrium and kinetic behavior can in principle be affected by relatively minor changes in either the calmodulin or target sequence. In addition, the striking effects of mutation on the individual calmodulin domains suggest a more general principle, namely, that small non-cross-linked proteins with appropriately small values of ΔH and ΔC_p can respond with great sensitivity to individual mutations. Such concepts may be valuable in introducing different degrees of thermostability into small proteins and protein domains. For a regulatory protein such as calmodulin, it suggests that the stability of both holo- and apo-forms of the protein needs to be strongly preserved to ensure the maintenance of biological function, and this is achieved through the high level of conservation of key residues, such as those involved in the short β-sheet region of each domain.

ACKNOWLEDGMENT

We thank Steve Howell for mass spectrometry and Peter Fletcher for peptide synthesis.

REFERENCES

Aitken, A., Howell, S., Jones, D., Madrazo, J., & Patel, Y. (1995) *J. Biol. Chem. 270,* 5706−5709.

Alexander, P., Fahenstock, S., Lee, T., Orban, J., & Bryan, P. (1992) *Biochemistry 31,* 3597−3603.

Axe, D. D., Foster, N. W., & Fersht, A. R. (1996) *Proc. Natl. Acad. Sci. U.S.A. 93,* 5590−5594.

Babu, A., Bugg, C. E., & Cook, W. J. (1988) *J. Mol. Biol. 204,* 191−204.

Bayley, P. M., & Martin, S. R. (1992) *Biochim. Biophys. Acta 1160,* 16−21.

Bayley, P. M., Findlay, W. A., & Martin, S. R. (1996) *Protein Sci. 5,* 1215−1228.

Becktel, W. J., & Schellman, J. A. (1987) *Biopolymers 26,* 1859−1877.

Brown, S. E., Martin, S. R., & Bayley, P. M. (1997) *J. Biol. Chem. 272,* 3389−3397.

Browne, J. P., Martin, S. R., & Bayley, P. M. (1996) *Biophys. J. 70,* A57.

Browne, J. P., Strom, M., Martin, S. R., & Bayley, P. M. (1997) *Biophys. J. 72,* A83.

Brzeska, H., Venyaminov, S. V., Grabarek, Z., & Drabikowski, W. (1983) *FEBS Letts. 153,* 169−173.

Crivici, A., & Ikura, M. (1995) *Annu. Rev. Biophys. Biomol. Struct. 24,* 85−116.

Eisenberg, D., Schwarz, E., Komaromy, M., & Wall, R. (1984) *J. Mol. Biol. 179,* 125−142.

Falke, J. J., Drake, S. K., Hazard, A. L., & Peersen, O. B. (1994) *Quart. Rev. Biophys. 27,* 219−290.

Findlay, W. A., Martin, S. R., Beckingham, K., & Bayley, P. M. (1995a) *Biochemistry 34,* 2087−2094.

Findlay, W. A., Gradwell, M. J., & Bayley, P. M. (1995b) *Protein Sci. 4,* 2375−2382.

Finn, B. E., Evenäs, J., Drakenberg, T., Waltho, J. P., Thulin, E., & Forsén, S. (1995) *Nat. Struct. Biol. 2,* 777−783.

Gill, S. C., & von Hippel, P. H. (1989) *Anal. Biochem. 182*, 319−326.
Haiech, J., Kilhoffer, M. C., Lukas, T. J., Craig, T. A., Roberts, T. M., & Watterson, D. M. (1991) *J. Biol. Chem. 266*, 3427−3431.
Ikura, M., Clore, G. M., Gronenborn, A. M., Zhu, G., Klee, C. B., & Bax, A. (1992) *Science 256*, 632−638.
Kawasaki, H., & Kretsinger, R. H. (1994) *Protein Profile 1*, 343−346.
Kilhoffer, M.-C., Demaille, J. G., & Gérard, D. (1981) *Biochemistry 20*, 4407−4414.
Klee, C. B. (1988) *Mol. Asp. Cell. Regul. 5*, 35−56.
Kubinowa, H., Tjandra, N., Grzesiek, S., Ren, H., Klee, C. B., & Bax, A. (1995) *Nat. Struct. Biol. 2*, 768−776.
Landt, O., Grunert, H.-P., & Hahn, U. (1990) *Gene 96*, 125−128.
Linse, S., Brodin, P., Johansson, C., Thulin, E., Grundström, T., & Forsén, S. (1988) *Nature 335*, 651−652.
Linse, S., Helmersson, A., & Forsén, S. (1991a) *J. Biol. Chem. 266*, 8050−8054.
Linse, S., Johansson, C., Brodin, P., Grundström, T., Drakenberg, T., & Forsén, S. (1991b) *Biochemistry 30*, 154−162.
Marsden, B. J., Shaw, G. S., & Sykes, B. D. (1990) *Biochem. Cell. Biol. 68*, 587−601.
Martin, S. R., & Bayley, P. M. (1986) *Biochem. J. 238*, 485−490.
Martin, S. R., Maune, J. F., Beckingham, K., & Bayley, P. M. (1992) *Eur. J. Biochem. 205*, 1107−1114.
Martin, S. R., Bayley, P. M., Brown, S. E., Porumb, T., Zhang, M., & Ikura, M. (1996) *Biochemistry 35*, 3508−3517.
Maune, J. F., Klee, C. B., & Beckingham, K. (1992a) *J. Biol. Chem. 267*, 5286−5295.
Maune, J. F., Beckingham, K., Martin, S. R., & Bayley, P. M. (1992b) *Biochemistry 31*, 7779−7786.
Meador, W. E., Means, A. R., & Quiocho, F. A. (1992) *Science 257*, 1251−1255.
Meador, W. E., Means, A. R., & Quiocho, F. A. (1993) *Science 262*, 1718−1721.
Meyer, D. F., Mabuchi, Y., & Grabarek, Z. (1996) *J. Biol. Chem. 271*, 11284−11290.
Myers, J. K., Pace, N. C., & Scholtz, J. M. (1995) *Protein Sci. 4*, 2138−2148.
Pace, C. N., Vajdos, F., Fee, L., Grimsley, G., & Gray, T. (1995) *Protein Sci. 4*, 2411−2423.
Putkey, J. A., Slaughter, G. R., & Means, A. R. (1985) *J. Biol. Chem. 260*, 4704−4712.
Reid, R. E., Gariépy, J., Saund, A. K., Hodges, R. S. (1981) *J. Biol. Chem. 256*, 2742−2751.
Richards, F. M., & Lim, W. A. (1993) *Q. Rev. Biophys. 26*, 423−498.
Sambrook, J., Fritsch, E. F., & Maniatis, T. (1989) *Molecular Cloning: A Laboratory Manual*, 2nd ed., Cold Spring Harbor Laboratory Press., Plainview, NY.
Schellman, J. A. (1987) *Annu. Rev. Biophys. Biophys. Chem. 16*, 115−137.
Smith, C. K., & Regan, L. (1995) *Science 270*, 980−983.
Smith, C. K., Withka, J. M., & Regan, L. (1994) *Biochemistry 33*, 5510−5517.
Starovasnik, M. A., Su, D. R., Beckingham, K., & Klevit, R. E. (1992) *Protein Sci. 1*, 245−253.
Strynadka, N. C. J., & James, M. N. G. (1989) *Annu. Rev. Biochem. 58*, 951−998.
Sturtevant, J. M. (1993) *Pure Appl. Chem. 65*, 991−998.
Tsalkova, T. N., & Privalov, P. L. (1985) *J. Mol. Biol. 181*, 533−544.
Zhang, M., Tanaka, T., & Ikura, M. (1995) *Nat. Struct. Biol. 2*, 758−767.

BI970460D